Widely tunable terahertz-wave generation in an organic crystal and its spectroscopic application

T. Taniuchi,[a] S. Okada, and H. Nakanishi
Institute of Multidisciplinary Research for Advanced Materials, Tohoku University 2-1-1 Katahira, Aoba-ku, Sendai 980-8577, Japan

Terahertz (THz)-wave generation using difference-frequency mixing in an organic 4-N, N-dimethylamino-4′-N′-methyl-stilbazolium tosylate (DAST) crystal was investigated theoretically and experimentally. We developed a dual-wavelength optical parametric oscillator (OPO) with two KTiOPO$_4$ crystals as the input light source. This oscillator has a tunable range from 1300–1450 nm and is pumped by a diode-pumped, frequency-doubled, Q-switched Nd:YAG laser with a pulse duration of 10 ns. Widely tunable THz waves ranging from 2 to 20 THz were generated from DAST crystals with 0.5- and 1-mm thickness using the OPO. THz output energies of 82 nJ (peak power of 10.3 W) at 11.6 THz and 110 nJ (peak power of 13.8 W) at 19 THz were obtained with a 1-mm-thick DAST crystal. Using a tunable THz-wave system consisting of the THz source and a pyroelectric detector, THz spectroscopic data for a polytetrafluoroethylene sheet were obtained and were comparable to data obtained from a conventional far-infrared spectrometer. © *2004 American Institute of Physics.* [DOI: 10.1063/1.1713045]

I. INTRODUCTION

Coherent tunable terahertz (THz) waves have great potential for frequency-domain spectroscopy and THz-imaging applications. Difference-frequency generation (DFG) using nonlinear optical (NLO) crystals has a wide tunability when the DFG crystal and the wavelengths of the input optical waves are correctly selected. For efficient THz-wave generation, the NLO crystal is required to have large nonlinear, low-absorption coefficients. Tunable THz waves from 0.3 to 7 THz have been generated using many inorganic NLO crystals, such as SiO$_2$ (quartz),[1] GaAs,[2] ZnTe,[3] LiNbO$_3$,[4] GaP,[5,6] GaSe,[7] and ZnGeP$_2$.[8] However, it is particularly difficult to generate waves with frequencies above 10 THz using inorganic NLO crystals due to strong phonon absorption.

Organic crystals with a large nonlinearity are promising candidates for wideband THz generation. The organic crystal 4-N, N-dimethylamino-4′-N′-methyl-stilbazolium tosylate (DAST)[9] has a large NLO coefficient (>200 pm/V) and a low dielectric constant,[10,11] which is advantageous for phase-matching optical waves and THz waves. Despite its superior properties for NLO interactions, DAST has not been used practically because it is difficult to grow such large and high-quality single crystals. Recently, Mori *et al.*[12] proposed the slope nucleation method for growing high-quality DAST crystals. This technique combines spontaneous nucleation and the subsequent growth of a single crystal into one process.

THz pulse radiation from thin DAST crystals using optical rectification of a femtosecond laser pulse has been reported.[13,14] Han *et al.*[15] demonstrated THz pulse radiation up to 15 THz by pumping a 0.1-mm-thick DAST crystal using a 15-fs pulse laser. Moreover, frequency-tunable THz waves have been generated from DAST crystals using a dual-wavelength Ti:Al$_2$O$_3$ laser[16] and an optical parametric oscillator (OPO).[17,18] Previously, we demonstrated continuously tunable THz-wave generation from 0.2 to 1.5 THz using a 1-mm-thick DAST crystal with a KTiOPO$_4$ (KTP)-based OPO near 1064 nm.[18] DAST is a promising material for the generation of THz waves below 1 THz because of its large NLO effect and low absorption loss. Recently, we also succeeded in generating high-frequency waves from 1.5 to 6.5 THz using a KTP-OPO in the 1150-nm range with a 0.2-mm-thick DAST crystal.[19]

In this paper, we report the properties of tunable THz-wave generation based on theoretical and experimental studies. By calculating the collinear phase-matching conditions, the wavelength range and the thickness of the DAST crystal can be determined theoretically. As the light source for collinear phase-matched DFG, we developed a dual-wavelength OPO at a 1300–1450 nm range by angle-tuning KTP crystals pumped at 532 nm. Widely tunable THz waves up to 20 THz were generated by mixing the OPO output with 0.5- and 1-mm-thick DAST crystals. THz spectroscopic data for a polytetrafluoroethylene sheet were obtained using the tunable THz-wave system consisting of the DFG-based THz-wave source and a pyroelectric detector and were comparable to data obtained from a conventional far-infrared spectrometer.

II. THEORETICAL CALCULATION

The THz output depends on the phase-matching conditions of DFG and the absorption of the crystal. The phase-matching conditions for the DFG interaction are given by

energy conservation:
$$\left| \frac{1}{\lambda_1} - \frac{1}{\lambda_2} \right| = \frac{1}{\lambda_3},$$

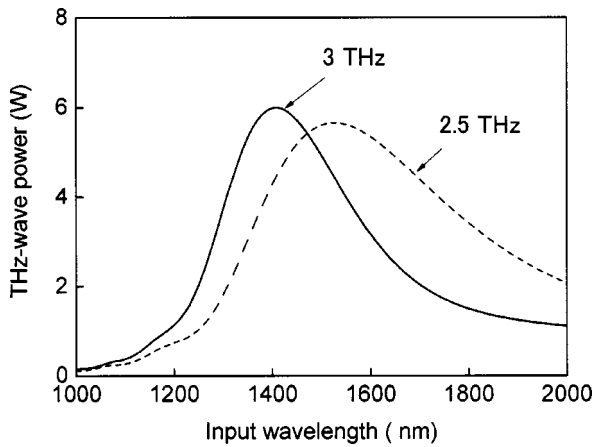$$(1)$$

[a] Electronic mail: taniuchi@tagen.tohoku.ac.jp

FIG. 1. The THz-wave power as a function of the input wavelength (λ_1). Solid line: 3 THz; broken line: 2.5 THz.
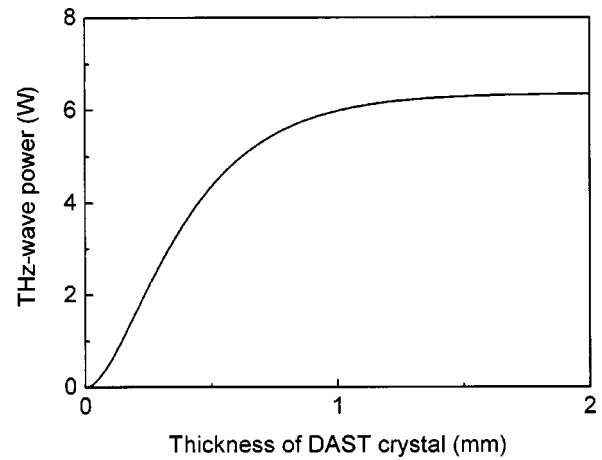

FIG. 2. The THz-wave power at 3 THz as a function of DAST thickness.

momentum conservation: $\left| \dfrac{n_1}{\lambda_1} - \dfrac{n_2}{\lambda_2} \right| = \dfrac{n_3}{\lambda_3},$

where λ_1 and λ_2 are the input wavelengths, λ_3 is the DFG wavelength, and n_1, n_2, and n_3 are the refractive indices at the respective wavelengths.

The output power of the THz wave obtained using DFG in the DAST crystal is given by the well-known formula,[20]

$$P_3 = \frac{2\omega_3^2 d_{11}^2 L^2}{\varepsilon_0 c^3 n_1 n_2 n_3} \left(\frac{P_1 P_2}{\pi r^2} \right) T_1 T_2 T_3 S,$$

$$S = \exp(-\alpha_3 L)$$

$$\cdot \frac{1 + \exp(-\Delta aL) - 2\exp(-\tfrac{1}{2}\Delta \alpha L)\cos(\Delta kL)}{(\Delta kL)^2 + (\tfrac{1}{2}\Delta \alpha L)^2},$$

$$\Delta k = k_1 - k_2 - k_3, \quad \Delta \alpha = |\alpha_1 - \alpha_2 - \alpha_3|, \quad (2)$$

where P_1 and P_2 are the input peak powers of the OPO, and P_3 is the peak THz power generated. L is the thickness of the DAST crystal. T_1, T_2, and T_3 are the Fresnel transmission coefficients, given by $T_j = 4n_j/(n_j+1)^2$, $j = 1, 2, 3$, and Δk is the momentum mismatch. α_1, α_2, and α_3 are the absorption coefficients. The subscripts $j = 1, 2,$ and 3 correspond to the frequencies of the OPO (ω_1 and ω_2) and the THz wave (ω_3). r is the radius of the OPO beam focal spot. The refractive indices n_1 and n_2 for the input light waves are given by the Sellmeier formula.[10] The refractive index n_3 and the absorption coefficient α_3 in the range of 0–3 THz were estimated from the data investigated by Walther et al.[21] using THz time-domain spectroscopy.

Figure 1 depicts the calculated THz-wave power as a function of the input wavelength λ_1 for generating 2.5- and 3-THz waves in a 1-mm-thick DAST crystal. For the theoretical calculation in Eqs. (1) and (2), we used the following data: $d_{11} = 210$ pm/V, $P_1 = P_2 = 30$ kW, $n_3 = 2.26$ (2.5 THz) or 2.30 (3 THz), $\alpha_1 = \alpha_2 = 0.5$ cm^{-1}, $\alpha_3 = 60$ cm^{-1} (2.5 THz) or 70 cm^{-1} (3 THz), and $r = 170$ μm. The appropriate wavelength λ_1 for 2.5 THz was found to be about 1530 nm, and 1400 nm for 3 THz from the figure. The result demon-

strates that phase matching is not so critical; a wavelength range of 1400–1500 nm can be used for efficient generation above 2 THz.

Figure 2 presents the calculated THz-wave power at 3 THz as a function of the DAST thickness using Eq. (2) with $\lambda_1 = 1450$ nm, $\lambda_2 = 1429$ nm, $n_1 = 2.140$, $n_2 = 2.142$. Because of the strong absorption, the THz-wave power does not increase monotonically with the DAST thickness, but becomes saturated when the DAST crystal is thicker than 1 mm. As a result of these calculations, the selected wavelengths of the input light waves close to 1450 nm were used in our experiment, with 0.5- and 1-mm thick DAST crystals.

III. EXPERIMENTAL RESULTS AND DISCUSSION

As a light source for THz-wave generation, we developed an OPO with dual wavelengths near 1450 nm using two KTP crystals in the same cavity. Idler waves in the range of 1300–1450 nm can be generated by angle-tuning a KTP crystal pumped at 532 nm in the XZ plane. Figure 3 shows the idler wavelengths calculated for the phase-matching condition in this configuration. To generate dual wavelengths in the range of 1300–1450 nm, we used two KTP crystals cut so that $\theta = 60°$. In this experiment, the angle of the first KTP was fixed to generate an idler wave at $\lambda_1 = 1450$ nm, and the
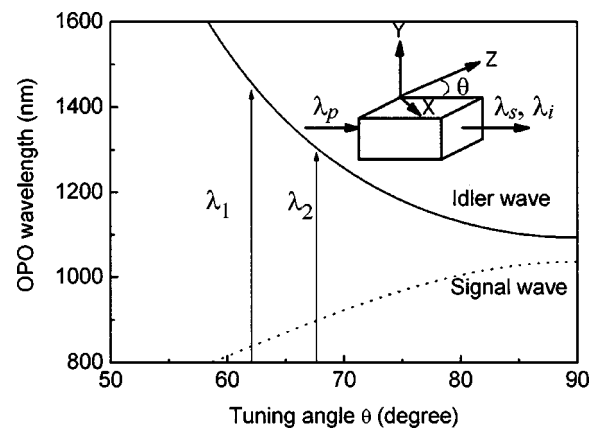

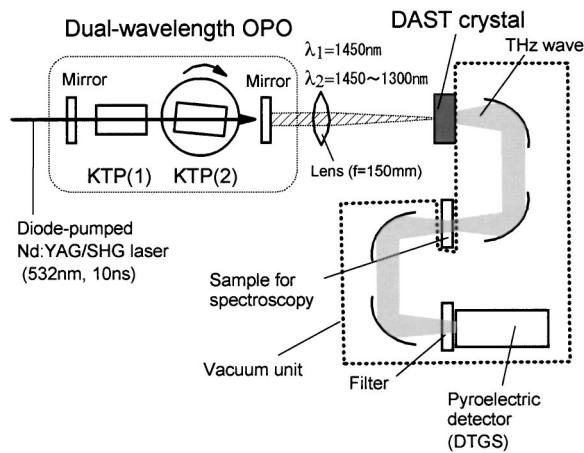FIG. 3. Angle tuning curves for KTP-OPO pumped at 532 nm.

FIG. 4. Schematic diagram of the experimental arrangement for THz-wave generation in DAST crystal.

FIG. 5. Wavelength dependence of the total OPO energy and a typical spectrum of the dual-wavelength OPO (inset).

second KTP was tuned at $\lambda_2 = 1450$ to 1300 nm ($\theta = 62 – 68°$) using a computer-controlled rotating stage.

Figure 4 presents a schematic diagram of the experimental arrangement for THz-wave generation in DAST crystals. We used high-quality $3 \times 3 \times 0.5$-mm and $5 \times 8 \times 1.0$-mm DAST crystals grown using the slope nucleation method. The two developed surfaces parallel to the crystallographic (001) plane of the DAST crystals were flat, and nonpolished as-grown DAST crystals were used for THz generation. The dual-wavelength OPO has two KTP crystals in the same 150-mm-long cavity and two flat mirrors with high reflectance for the signal waves and high transmittance for the idler waves. The signal wavelength was 840 to 900 nm, which corresponds to an idler wavelength of 1300 to 1450 nm. We used $8 \times 5 \times 15$-mm flux-grown KTP crystals in this experiment. The pump source for the OPO was a diode-pumped, frequency-doubled, Q-switched Nd:YAG laser, with a pulse duration of 10 ns and a 20 Hz repetition rate. The threshold energy of the KTP-OPO was 3 mJ. An output energy of 0.55 to 0.7 mJ was obtained with a 9 mJ pump. The output beam of the OPO was focused on a 0.34-mm-diam spot on the DAST using a 150-mm focal-length lens.

The THz wave was collimated and focused with off-axis parabolic mirrors ($f = 25.4$ mm) and was detected by a deuterated triglycine sulfate (DTGS) pyroelectric crystal that was 2.5 mm in diam, operated at room temperature. The DTGS detector used in this experiment was made by JASCO for a far-infrared spectrometer. A black polyethylene filter was used to block any optical waves. The maximum THz-wave output was obtained when the polarization of the input optical waves paralleled the a axis of the DAST crystal. To avoid water-vapor absorption, the parabolic mirrors and detector were inserted in a vacuum unit (10^{-3} Torr).

Figure 5 illustrates the wavelength dependence of the total OPO energy. In this experiment, λ_1 was fixed at 1450 nm, and λ_2 was varied from 1445 to 1300 nm, which corresponded to frequency tuning from 0.7 to 25 THz. The output energy slowly changed from 0.55 to 0.7 mJ due to the reflectance properties of the OPO mirrors and the angle-tuning dependence of the effective NLO coefficient of the KTP crystal. The inset in the figure shows a typical spectrum of
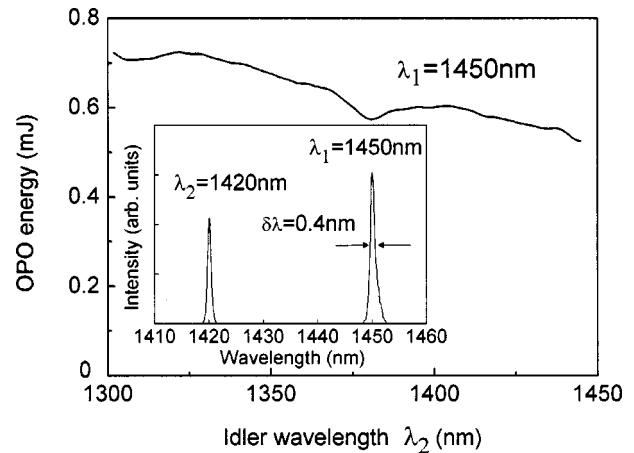
the dual-wavelength OPO. The spectral bandwidth of both wavelengths was around 0.4 nm. The output power at λ_2 was slightly less than that at λ_1 due to pump depletion. The spectral bandwidth did not change throughout the tuning range.

Figure 6 illustrates the THz-wave energy generated as a function of the THz frequency with 0.5- and 1-mm thick DAST crystals. Continuously tunable THz waves from 2 to 20 THz were generated in both samples with the same peak frequencies of 2.5, 4.5, 11.6, and 19 THz. The output energies of the THz waves were 22 nJ/pulse at 2.5 THz, 82 nJ/pulse at 11.6 THz, and 110 nJ/pulse at 19 THz. Since the pulse duration of the OPO was about 8 ns, the peak power of the THz wave was estimated to be 2.8 W at 2.5 THz, 10.3 W at 11.6 THz, and 13.8 W at 19 THz. As the energies of the THz waves were obtained over a range exceeding 0.3 nJ, which was the noise level of the detector, the pyroelectric detector could be used with a high signal-to-noise ratio without using a Si bolometer operating at 4 K.

As shown, THz peaks and dips have the same frequencies for both DAST samples. These properties were the same when λ_1 was varied from 1350 to 1450 nm. Therefore, they do not correspond to the phase-matching condition, due to
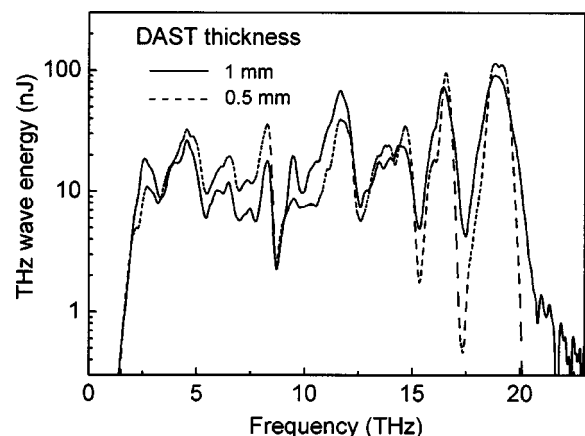

FIG. 6. THz output energy as a function of the THz frequency with 1- and 0.5-mm-thick DAST crystals. Solid line: 1 mm DAST; broken line: 0.5 mm DAST.

the molecular properties of the DAST crystal. The frequency dips at 3.1, 5.2, 8.5, 15.2, and 17.3 THz are thought to be due to the absorption of the DAST crystal.[22] The decrease below 2 THz is because of the strong absorption in DAST corresponding to the resonance of the transverse optical phonon at 1.1 THz.[21] Conversely, the decrease above 19 THz is due to the crystalline nature of the DAST crystal and to the strong absorption by the black polyethylene filter.

The output energy at 2.5 THz for the 1-mm sample is about two times higher than that of the 0.5 mm sample. This difference is thought to occur because the THz power in the low-loss region below 3 THz increases with the thickness of the DAST crystal, as shown in Fig. 2. Conversely, in the high-loss region above 3 THz, the THz output energy does not increase with the thickness due to saturation, but depends on the quality of the DAST crystal. Considering the decrease in THz waves at 15.2 and 17.3 THz, DAST crystals about 1 mm thick are better as a wideband THz source for spectroscopy and imaging applications than those in the 0.5-mm sample.

A theoretical value of THz peak power $P_3 = 6.7$ W at 2.5 THz was obtained from Eq. (2), using $P_1 = 45$ kW (0.36 mJ/8 ns) and $P_2 = 30$ kW (0.24 mJ/8 ns). Under the same conditions, our experimental result was $P_3 = 2.8$ W. This is consistent with the calculation results, considering the 55% loss in the THz-wave collimation system. The normalized conversion efficiency $P_3/(P_1 P_2)$ was estimated to be 2 $\times 10^{-9}$/W. In a previous paper,[16] we found the conversion efficiency was $P_3/(P_1 P_2) \sim 10^{-14}$/W at 1.4 THz using the dual-wavelength Ti:Al$_2$O$_3$ laser. The conversion efficiency obtained in this experiment was about 10^5 higher than the previous value. The reason for the efficient THz-wave generation in our system is thought to be the use of the high-quality DAST crystal under phase-matching conditions.

For time-domain spectroscopy using high-frequency radiation above 10 THz, it is necessary to use an expensive ultrafast laser below 15 fs. THz imaging particularly requires a high-power laser with a regenerative amplifier exceeding 1 mJ. By contrast, THz waves above 10 THz can be generated in the DFG scheme using the same nanosecond laser as for 3-THz generation. Therefore, a DFG-based tunable THz source has a great advantage over a THz pulse source for THz imaging in the high-frequency region above 10 THz.

Using our tunable THz source, we measured the transmittance of a polytetrafluoroethylene (PTFE) sheet in the range of 2–15 THz as an example of THz frequency-domain spectroscopy. Figure 7 compares the transmittance of a 0.2-mm-thick PTFE sheet measured using the tunable THz source and a conventional far-infrared spectrometer with a 2-cm^{-1} resolution. We observed a strong absorption band at 6.1 THz (203 cm^{-1}), which was attributed to the CF$_2$ twisting vibration of the PTFE.[23] These results indicate that a tunable THz source with DAST can be used for wideband THz spectroscopy. The estimated bandwidth of the THz waves that were generated was about 60 GHz (2 cm^{-1}), which corresponds to an optical spectral bandwidth of 0.4 nm. To generate a narrow THz wave for high-resolution spectroscopic applications, the spectral bandwidth of the
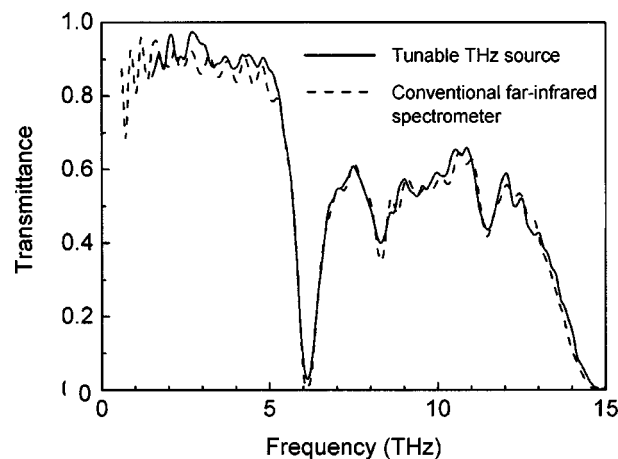

FIG. 7. Comparison of the transmittance of a PTFE sheet using a tunable THz source (solid line) and a conventional far-infrared spectrometer (broken line).

KTP-OPO can be narrowed by inserting a grating element into the OPO cavity.

IV. CONCLUSION

We investigated THz-wave generation from DAST crystals theoretically and experimentally. The wavelength range and thickness of DAST crystals for efficient DFG can be determined from calculating the collinear phase-matching conditions. Widely tunable THz waves from 2 to 20 THz were generated by mixing the output of an OPO over the 1300–1450 nm range. The frequency of the THz wave was continuously tuned by changing the KTP crystal angle in the OPO cavity. In this study, the output energies of the THz waves were as high as 82 nJ/pulse (peak power of 10.3 W) at 11.6 THz and 110 nJ/pulse (peak power of 13.8 W) at 19 THz. Using a tunable THz-wave system consisting of a DFG-based THz-wave source and a pyroelectric detector, we obtained spectroscopic data for a PTFE sheet and found it comparable to the data obtained from a conventional far-infrared spectrometer. Therefore, our system should also be useful for practical THz imaging, THz sensing, and spectroscopic applications. In addition, tunable THz-wave generation with higher energy and a wider frequency range is expected to use more perfect DAST crystals.

ACKNOWLEDGMENTS

[1] F. Zernike, Jr. and P. R. Berman, Phys. Rev. Lett. **15**, 999 (1965).
[2] R. L. Aggarwal, B. Lax, H. R. Fetterman, P. E. Tannenwald, and B. J. Clifton, J. Appl. Phys. **45**, 3972 (1974).
[3] T. Yajima and K. Inoue, IEEE J. Quantum Electron. **QE-5**, 140 (1969).
[4] K. H. Yang, J. R. Morris, P. L. Richards, and Y. R. Shen, Appl. Phys. Lett. **23**, 669 (1973).
[5] F. De Martini, Phys. Rev. B **4**, 4556 (1971).
[6] T. Tanabe, K. Suto, J. Nishizawa, K. Saito, and T. Kimura, Appl. Phys. Lett. **83**, 237 (2003).

[7] W. Shi, Y. J. Ding, N. Fernelius, and K. Vodopyanov, Opt. Lett. **27**, 1454 (2002).

[8] W. Shi and Y. J. Ding, Appl. Phys. Lett. **83**, 848 (2003).

[9] H. Nakanishi, H. Matsuda, S. Okada, and M. Kato, Proceedings of the MRS International Meeting on Advanced Materials **1**, 97 (1989).

[10] U. Meier, M. Bosch, Ch. Bosshard, F. Pan, and P. Gunter, J. Appl. Phys. **83**, 3486 (1998).

[11] F. Pan, G. Knople, Ch. Bosshard, S. Follonier, R. Spreiter, M. S. Wong, and P. Gunter, Appl. Phys. Lett. **69**, 13 (1996).

[12] Y. Mori, Y. Takahashi, T. Iwai, M. Yoshimura, Y. K. Yap, and T. Sasaki, Jpn. J. Appl. Phys. **39**, L1006 (2000).

[13] X.-C. Zhang, X. F. Ma, Y. Jin, T.-M. Lu, E. P. Boden, P. D. Phelps, K. R. Stewart, and C. P. Yakymyshyn, Appl. Phys. Lett. **61**, 3080 (1992).

[14] T. J. Carrig, G. Rodriquez, T. S. Clement, and K. R. Stewart, Appl. Phys. Lett. **66**, 10 (1995).

[15] P. Y. Han, M. Tani, F. Pan, and X.-C. Zhang, Opt. Lett. **25**, 675 (2000).

[16] K. Kawase, M. Mizuno, S. Souma, H. Takahashi, T. Taniuchi, Y. Urata, S. Wada, H. Tashiro, and H. Ito, Opt. Lett. **24**, 1065 (1999).

[17] K. Kawase, T. Hatanaka, H. Takahashi, K. Nakamura, T. Taniuchi, and H. Ito, Opt. Lett. **25**, 1714 (2000).

[18] T. Taniuchi, J. Shikata, and H. Ito, Electron. Lett. **36**, 1414 (2000).

[19] T. Taniuchi, J. Shikata, N. Osaki, and H. Ito, Proceedings of the Conference on Lasers and Electro-Optic (CLEO'2002), CTuC5, 148 (2002).

[20] R. L. Aggarwal and B. Lax, in *Nonlinear Infrared Generation* (Springer, New York, 1977), p. 28.

[21] M. Walther, K. Jensby, S. R. Keiding, H. Takahashi, and H. Ito, Opt. Lett. **25**, 911 (2000).

[22] Ch. Bosshard, R. Spreiter, L. Degiorgi, and P. Gunter, Phys. Rev. B **66**, 205 107 (2002).

[23] P. Dannetun, M. Scott, and M. Rei Vilar, Thin Solid Films **286**, 321 (1996).